POWER SYSTEM STATE ESTIMATION VIA FEASIBLE POINT PURSUIT

Gang Wang, Ahmed S. Zamzam, Georgios B. Giannakis, and Nicholas D. Sidiropoulos

Dept. of ECE and Digital Tech. Center
Univ. of Minnesota, Minneapolis, MN 55455
Emails: {gangwang,ahmedz,georgios,nikos}@umn.edu

ABSTRACT

Power system state estimation (PSSE) is a critical task for grid operation efficiency and system stability. Physical laws dictate quadratic relationships between observable quantities and voltage state variables, hence rendering the PSSE problem nonconvex and *NP-hard*. Existing SE solvers largely rely on iterative optimization methods or semidefinite relaxation (SDR) techniques. Even when based on noiseless measurements, convergence of the former is sensitive to the initialization, while the latter is challenged by small-size measurements especially when voltage magnitudes are not available at all buses. At the price of running time, this paper proposes a novel *feasible point pursuit* (FPP)-based SE solver, which iteratively seeks feasible solutions for a nonconvex quadratically constrained quadratic programming reformulation of the weighted least-squares (WLS) SE problem. Numerical tests corroborate that the novel FPP-based SE markedly improves upon the Gauss-Newton based WLS and SDR-based SE alternatives, also when noisy measurements are available.

Index Terms— Power system state estimation, nonconvex QCQP, feasible point pursuit

1. INTRODUCTION

The task of *power system state estimation* (PSSE) amounts to estimating the complex voltages at all buses across the network from a subset of supervisory control and data acquisition (SCADA) measurements including (active/reactive) power injections and flows as well as voltage magnitudes [1, 2]. Since its appearance in the 1970s [1], PSSE has become a prerequisite for supervisory control, system planning, and economic dispatch [1–4]. Nevertheless, nonlinear SCADA measurements render the PSSE problem nonconvex [5] and *NP-hard* in its general form.

Existing SE approaches rely on Gauss-Newton based weighted least-squares (WLS) and semidefinite relaxation (SDR)-based SE algorithms. The 'workhorse' Gauss-Newton method for nonconvex objectives comes with two limitations [6, Sec. 1.5]: sensitivity to initial guess and no convergence guarantees. SDR-based approaches on the other hand rely on the matrix-lifting technique that leads to a computationally expensive semidefinite program [5,7,8]. Performance of SDR-based solvers degrades when the number of measurements is small, or when the data do not include all nodal voltage magnitudes.

Recently, a feasible point pursuit-successive convex approximation (FPP-SCA) algorithm developed in [9] was advocated for solving the nonconvex optimal power flow (OPF) problem [10]. Empirically, the FPP-based OPF solver was shown to achieve improved performance over the SDR-based and moment relaxation-based OPF solvers in most IEEE benchmark systems [10, 11].

Building on [5, 10] and inspired by the nonconvexity challenge of PSSE, the goal of this paper is to develop a polynomial-time SE solver for AC power networks, which also features competitive statistical performance. To this end, the SE task is first formulated as a WLS problem. To leverage the FPP algorithm, the latter is converted to an equivalent nonconvex QCQP, which is subsequently tackled by FPP, yielding our FPP-based SE solver. Regarding notation, all matrices (vectors) are denoted by boldface letters, while $(\cdot)^{\mathcal{T}}$ and $(\cdot)^{\mathcal{H}}$ stand for transpose and complex-conjugate transpose, respectively.

2. PROBLEM FORMULATION

Consider a power transmission network comprising N buses. The network can be modeled as a graph $\mathcal{G} := \{\mathcal{N}, \mathcal{E}\}$, where $\mathcal{N} := \{1, 2, \ldots, N\}$ is the set of all nodes (buses), and $\mathcal{E} := \{(m, n)\} \subset \mathcal{N} \times \mathcal{N}$ the set of all edges (transmission lines). For every bus $n \in \mathcal{N}$, let $V_n := |V_n|e^{j\theta_n}$ denote its complex voltage, $I_n := |I_n|e^{j\phi_n}$ its complex current injection, and $S_n := P_n + jQ_n$ its complex power injection with P_n and Q_n being the active and reactive power injections, respectively. For each line $(m, n) \in \mathcal{E}$, let I_{mn} be the complex current flowing from bus m to n, and $S_{mn} := P_{mn} + jQ_{mn}$ the complex power flow from bus m to n seen at its sending end, where P_{mn} and Q_{mn} are the active and reactive power flow, respectively. For notational brevity, collect nodal quantities $\{V_n\}$, $\{I_n\}$, $\{P_n\}$, and $\{Q_n\}$ into vectors $\mathbf{v} := [V_1 \cdots V_N]^{\mathcal{T}} \in \mathbb{C}^N$, $\mathbf{i} := [I_1 \cdots I_N]^{\mathcal{T}} \in \mathbb{C}^N$,

The work of G. Wang and G. B. Giannakis was supported by NSF grants 1423316, 1442686, 1508993, and 1509040. The work of A. S. Zamzam and N. D. Sidiropoulos was partially supported by NSF under grants 1231504 and 1525194.

$\mathbf{p} := [P_1 \ \cdots \ P_N]^\mathcal{T} \in \mathbb{R}^N$, and $\mathbf{q} := [Q_1 \ \cdots \ Q_N]^\mathcal{T} \in \mathbb{R}^N$, respectively.

To estimate the voltage state vector $\mathbf{v}$, a total of L SCADA measurements are taken. Typically, SCADA has available the following types of measurements: squared voltage magnitude $|V_n|^2$, active (reactive) power injection P_n (Q_n), as well as active (reactive) power flow P_{mn} (Q_{mn}). With $\mathcal{N}_V$, $\mathcal{N}_P$, $\mathcal{N}_Q$, $\mathcal{E}_P$, and $\mathcal{E}_Q$ denoting the subsets of buses or lines where the actual (possibly noisy) measurements of the associated type are taken, all measurements can be stacked into an $L \times 1$ vector $\mathbf{z} := \big[\{|V_n|^2\}_{n\in\mathcal{N}_V}, \ \{P_n\}_{n\in\mathcal{N}_P}, \ \{Q_n\}_{n\in\mathcal{N}_Q}, \ \{P_{mn}\}_{(m,n)\in\mathcal{E}_P}, \ \{Q_{mn}\}_{(m,n)\in\mathcal{E}_Q}\big]^\mathcal{T} \in \mathbb{R}^{L\times 1}$.

The AC power flow model asserts that $\{z_\ell\}$s are quadratically related to $\mathbf{v}$. Apparently, this holds true for squared voltage magnitude measurements given as $|V_n|^2 = V_n V_n^\mathcal{H}$. To specify the relationship between power measurements and $\mathbf{v}$, letting $\mathbf{Y} \in \mathbb{C}^{N\times N}$ be the so-termed bus admittance matrix, the multivariate Ohm's law reads as [2]

$$\mathbf{i} = \mathbf{Y}\mathbf{v}. \tag{1}$$

Note that the symmetric but non-Hermitian matrix $\mathbf{Y}$ is sparse, thus enabling efficient computations, and its (m,n)-th entry is given by

$$Y_{mn} := \begin{cases} -y_{mn}, & (m,n) \in \mathcal{E} \\ \overline{y}_{nn} + \sum_{k\in\mathcal{N}_n} y_{nk}, & m = n \\ 0, & \text{otherwise} \end{cases} \tag{2}$$

where y_{mn} is the admittance of line $(m,n) \in \mathcal{E}$, $\overline{y}_{nn}$ the admittance to the ground at bus $n \in \mathcal{N}$, and $\mathcal{N}_n$ the set of neighboring buses directly connected to bus n. Let $\overline{y}_{mn}$ for $m \neq n$ denote the shunt admittance at bus m corresponding to line (m,n). Appealing to Ohm's and Kirchhoff's laws, the current flowing from bus m to n is expressed as

$$I_{mn} = \overline{y}_{mn} V_m + y_{mn}(V_m - V_n) \tag{3}$$

and the reverse-direction current I_{nm} can be given symmetrically. Because $\overline{y}_{mn} \neq 0$, it holds that $I_{mn} \neq -I_{nm}$.

The AC power flow model also confirms that $P_n + jQ_n = V_n I_n^\mathcal{H}$ holds $\forall n \in \mathcal{N}$. Appealing again to Ohm's law in (1), one arrives at the following matrix-vector representation

$$\mathbf{p} + j\mathbf{q} = \mathrm{diag}(\mathbf{v})\mathbf{i}^\mathcal{H} = \mathrm{diag}(\mathbf{v})\mathbf{Y}^\mathcal{H}\mathbf{v}^\mathcal{H} \tag{4}$$

where $\mathrm{diag}(\mathbf{v})$ is a diagonal matrix holding entries of $\mathbf{v}$ on its diagonal. Similar to active/reactive power injections, the sending-end active and reactive power flow from bus m to n can be expressed as

$$\begin{aligned} P_{mn} + jQ_{mn} &= V_m I_{mn}^\mathcal{H} \\ &= \left(\overline{y}_{mn}^\mathcal{H} + y_{mn}^\mathcal{H}\right) V_m V_m^\mathcal{H} - y_{mn}^\mathcal{H} V_m V_n^\mathcal{H} \end{aligned} \tag{5}$$

where the second equation arises from plugging I_{mn} into (3). Observe from (4) and (5) that (real/reactive) power injections and flows are expressible as quadratic functions of $\mathbf{v}$ as well.

Given this quadratic relationship, all (noiseless) measurements can be written as $z_\ell := \mathbf{v}^\mathcal{H}\mathbf{H}_\ell\mathbf{v}$ for $\ell = 1, \ldots, L$ [5], where the coefficient matrices $\{\mathbf{H}_\ell \in \mathbb{C}^{n\times n}\}$ will be specified shortly. In this direction, let $\left\{\mathbf{e}_n \in \mathbb{R}^{n\times 1}\right\}_{n=1}^N$ be the canonical basis of $\mathbb{R}^N$, and introduce further the following admittance-related matrices

$$\mathbf{Y}_n := \mathbf{e}_n\mathbf{e}_n^\mathcal{T}\mathbf{Y} \tag{6a}$$

$$\mathbf{Y}_{mn} := (\overline{y}_{mn} + y_{mn})\mathbf{e}_m\mathbf{e}_m^\mathcal{T} - y_{mn}\mathbf{e}_m\mathbf{e}_n^\mathcal{T}. \tag{6b}$$

Regarding the squared voltage magnitudes, since $|V_n|^2 = V_n V_n^\mathcal{H} = \mathbf{v}^\mathcal{H}\mathbf{e}_n\mathbf{e}_n^\mathcal{T}\mathbf{v}$, the corresponding $\{\mathbf{H}_\ell\}$ is given by

$$\mathbf{H}_{V,n} := \mathbf{e}_n\mathbf{e}_n^\mathcal{T} \succeq \mathbf{0}, \ \forall n. \tag{7}$$

Likewise, by taking real/imaginary parts of (4) and (5), the $\{\mathbf{H}_\ell\}$ associated with the active/reactive power injections and flows can be obtained as

$$\mathbf{H}_{P,n} := \frac{1}{2}\left(\mathbf{Y}_n + \mathbf{Y}_n^\mathcal{H}\right), \qquad \mathbf{H}_{Q,n} := \frac{j}{2}\left(\mathbf{Y}_n - \mathbf{Y}_n^\mathcal{H}\right)$$

$$\mathbf{H}_{P,mn} := \frac{1}{2}\left(\mathbf{Y}_{mn} + \mathbf{Y}_{mn}^\mathcal{H}\right), \ \mathbf{H}_{Q,mn} := \frac{j}{2}\left(\mathbf{Y}_{mn} - \mathbf{Y}_{mn}^\mathcal{H}\right).$$

When noise is accounted for, all measurements can be written as

$$z_\ell = \mathbf{v}^\mathcal{H}\mathbf{H}_\ell\mathbf{v} + \epsilon_\ell, \qquad \ell = 1, \ldots, L \tag{9}$$

where ϵ_ℓ denotes the zero-mean measurement noise with known variance σ_ℓ^2, henceforth assumed independent across meters and concatenated into the $L \times 1$ vector $\boldsymbol{\sigma}^2 := [\sigma_1^2 \ \cdots \ \sigma_L^2]^\mathcal{T}$. All $\{\mathbf{H}_\ell\}$ are Hermitian, but non-definite in general, except those corresponding to squared voltage magnitudes [cf. (7)].

The goal of SE is to estimate $\mathbf{v} \in \mathbb{C}^n$ from (possibly noisy) measurements $\mathbf{z} \in \mathbb{R}^L$. Adopting the WLS criterion, the SE task can be formulated as that of solving the nonlinear least-squares

$$\hat{\mathbf{v}} := \arg\min_{\mathbf{v}\in\mathbb{C}^N} \sum_{\ell=1}^L w_\ell \left(z_\ell - \mathbf{v}^\mathcal{H}\mathbf{H}_\ell\mathbf{v}\right)^2 \tag{10}$$

where the ℓ-th entry of the weight vector $\mathbf{w} := [w_1 \ \cdots \ w_L]^\mathcal{T}$ is typically chosen as $w_\ell := 1/\sigma_\ell^2$. The WLS estimate $\hat{\mathbf{v}}$ coincides with the maximum likelihood estimate of $\mathbf{v}$ when $\boldsymbol{\epsilon} := [\epsilon_1 \ \cdots \ \epsilon_L]^\mathcal{T}$ follows the multivariate normal distribution $\mathcal{N}(\mathbf{0}, \mathrm{diag}(\boldsymbol{\sigma}^2))$. Unfortunately, due to the quadratic terms, the SE problem in (10) is nonconvex [5]. Minimizing nonconvex objectives, which may exhibit many stationary points, is in general NP-hard [12]. In a nutshell, solving the problem in (10) is challenging.

Existing SE algorithms fall under two categories: convex and nonconvex ones. The latter includes the 'workhorse' Gauss-Newton method, which is typically employed in practice: Upon linearizing the error function in the LS cost about

a given estimate, the minimizer of the norm of the resulting linearized function is used to initialize the next iteration [6, Sec. 1.5]. Nevertheless, for nonconvex objective functions, the Gauss-Newton method is challenged by i) sensitivity to the initial estimate; and, ii) no convergence guarantee to even a stationary point [6]. Convex approaches based on SDR [5] express all (noiseless) measurements $\{z_\ell\}$ as linear functions of the outer-product $\mathbf{V} := \mathbf{v}\mathbf{v}^{\mathcal{H}}$. Then, the cost in (10) is convexified by dropping the nonconvex rank constraint $\mathrm{rank}(\mathbf{V}) = 1$. SDR-based SE seldom produces rank-1 solutions in the noisy setup. Additional eigen-decomposition or randomization procedures are required to recover a vector solution $\hat{\mathbf{v}}$ from the SDR solution $\hat{\mathbf{V}}$. Performance of SDR-based algorithms degrades when the number of measurements is small, or when the measurements do not include all nodal voltage magnitudes, as will be demonstrated by our numerical results in Section 4.

3. FEASIBLE POINT PURSUIT BASED SE SOLVER

The FPP algorithm was originally proposed in [9] for solving nonconvex QCQPs. FPP is an iterative algorithm which solves a sequence of convexified QCQPs instead. Per iteration, the nonconvex feasibility set is replaced by a convex inner approximation around a given point obtained by linear restriction. To ensure feasibility of the resulting convexified QCQP subproblems, a slack variable is introduced for each relaxed constraint, while penalization on the slack variable is imposed to enforce solutions of minimal constraint violation. The minimizer of the subproblem is then used as the linearization point of the next iteration.

Recall that the objective function in (10) is a quartic polynomial of $\mathbf{v}$, which can be re-written as

$$\min_{\mathbf{v},\,\{s_\ell\}_{l=1}^{L}} \quad \sum_{l=1}^{L} w_\ell s_\ell^2$$
$$\text{s.t.} \quad \left|z_\ell - \mathbf{v}^{\mathcal{H}}\mathbf{H}_\ell\mathbf{v}\right| \le s_\ell,\ \forall \ell = 1,\ldots,L \qquad (11a)$$

where $\mathbf{s} := \{s_\ell \ge 0\}_{\ell=1}^{L}$ are slack variables that relate to the deviations between (possibly noisy) measurements $\{z_\ell\}$ and the induced ones $\{\mathbf{v}^{\mathcal{H}}\mathbf{H}_\ell\mathbf{v}\}$. Problem (11) is equivalent to (10), as can be easily shown by contradiction. The constraints (11a) can be replaced by two sets of inequalities to yield a QCQP in the following form

$$\min_{\mathbf{v},\,\mathbf{s}} \quad \sum_{l=1}^{L} w_\ell s_\ell^2$$
$$\text{s.t.} \quad \mathbf{v}^{\mathcal{H}}\mathbf{H}_\ell\mathbf{v} \le z_\ell + s_\ell,\ \forall \ell = 1,\ldots,L \qquad (12a)$$
$$\mathbf{v}^{\mathcal{H}}\left(-\mathbf{H}_\ell\right)\mathbf{v} \le -z_\ell + s_\ell,\ \forall \ell = 1,\ldots,L \qquad (12b)$$

which remains nonconvex even for definite $\mathbf{H}_\ell$'s. Along the lines of FPP, the quadratic terms in (12a) are decomposed into its convex and nonconvex components as

$$\mathbf{v}^{\mathcal{H}}\mathbf{H}_\ell^{(+)}\mathbf{v} + \mathbf{v}^{\mathcal{H}}\mathbf{H}_\ell^{(-)}\mathbf{v} \le z_\ell + s_\ell \qquad (13)$$

with $\mathbf{H}_\ell^{(+)}$ and $\mathbf{H}_\ell^{(-)}$ being the positive and negative semidefinite components of $\mathbf{H}_\ell$, respectively. For $\mathbf{H}_\ell^{(-)} \preceq \mathbf{0}$ in (13), it holds that

$$(\mathbf{v}-\mathbf{y})^{\mathcal{H}}\mathbf{H}_\ell^{(-)}(\mathbf{v}-\mathbf{y}) \le 0,\ \forall \mathbf{y} \in \mathbb{C}^n$$

which after expanding the left-hand-side yields

$$\mathbf{v}^{\mathcal{H}}\mathbf{H}_\ell^{(-)}\mathbf{v} \le 2\,\mathrm{Re}\Big\{\mathbf{y}^{\mathcal{H}}\mathbf{H}_\ell^{(-)}\mathbf{v}\Big\} - \mathbf{y}^{\mathcal{H}}\mathbf{H}_\ell^{(-)}\mathbf{y}.$$

Key to FPP is replacing nonconvex terms associated with $\mathbf{H}_\ell^{(-)}$ by their inner linear approximation around a given $\mathbf{y}$ yielding

$$\mathbf{v}^{\mathcal{H}}\mathbf{H}_\ell^{(+)}\mathbf{v} + 2\,\mathrm{Re}\Big\{\mathbf{y}^{\mathcal{H}}\mathbf{Y}_k^{(-)}\mathbf{v}\Big\} \le z_\ell + \mathbf{y}^{\mathcal{H}}\mathbf{H}_\ell^{(-)}\mathbf{y} + s_\ell. \quad (14)$$

In the same fashion, (12b) is replaced by

$$\mathbf{v}^{\mathcal{H}}\left(-\mathbf{H}_\ell^{(-)}\right)\mathbf{v} - 2\,\mathrm{Re}\Big\{\mathbf{y}^{\mathcal{H}}\mathbf{H}_\ell^{(+)}\mathbf{v}\Big\} \le -z_\ell - \mathbf{y}^{\mathcal{H}}\mathbf{H}_\ell^{(+)}\mathbf{y} + s_\ell. \quad (15)$$

The minimum values required for the slacks $\{s_\ell\}$ to satisfy (14) and (15) depend on the noise contained in $\{z_\ell\}$. Replacing the nonconvex constraints with their convex surrogates, an upper bound on the fitting error is minimized by penalizing the weighted sum of squares of the slack variables.

Upon obtaining the $\mathbf{v}$-minimizer at the i-th iteration $\mathbf{v}_i$, our FPP-based SE algorithm amounts to solving the following convexified QCQP subproblem at the $(i+1)$-th iteration

$$\{\mathbf{v}_{i+1}, \mathbf{s}_{i+1}\} := \arg\min_{\mathbf{v},\,\mathbf{s}} \quad \sum_{l=1}^{L} w_\ell s_\ell^2 \qquad (16a)$$

s.t.

$$\mathbf{v}^{\mathcal{H}}\mathbf{H}_\ell^{(+)}\mathbf{v} + 2\,\mathrm{Re}\Big\{\mathbf{y}^{\mathcal{H}}\mathbf{H}_\ell^{(-)}\mathbf{v}\Big\} \le z_\ell + \mathbf{y}^{\mathcal{H}}\mathbf{H}_\ell^{(-)}\mathbf{y} + s_\ell,$$
$$\forall \ell = 1,\ldots,L \quad (16b)$$
$$\mathbf{v}^{\mathcal{H}}\mathbf{H}_\ell^{(-)}\mathbf{v} + 2\,\mathrm{Re}\Big\{\mathbf{y}^{\mathcal{H}}\mathbf{H}_\ell^{(+)}\mathbf{v}\Big\} \ge z_\ell + \mathbf{y}^{\mathcal{H}}\mathbf{H}_\ell^{(+)}\mathbf{y} - s_\ell,$$
$$\forall \ell = 1,\ldots,L \quad (16c)$$

where $\mathbf{y} := \mathbf{v}_i$ is the $\mathbf{v}$-minimizer of (16) at the i-th iteration.

Two observations are in order. Minimizing the slack variable's square associated with a certain measurement, the corresponding fitting error is minimized. Note also that the convex QCQP in (16) can be solved efficiently using off-the-shelf solvers. Our FPP-based SE solver is summarized in Algorithm 1 next.

4. SIMULATED TESTS

Numerical tests comparing the proposed FPP-based SE approach with the WLS method using Gauss-Newton iterations (GN-based SE) and the SDR-based SE algorithms [5] are presented in this section. Performance is evaluated in terms of the normalized root mean-square error, defined as

Algorithm 1: FPP-based PSSE Solver

Initialization: set $i = 0$ and $\mathbf{y}$ to be the flat-voltage point.
repeat
  $\mathbf{v}_i, \{s_\ell\}_{\ell=1}^{L} \leftarrow$ solution of problem (16).
  $\mathbf{y} \leftarrow \mathbf{v}_i$.
  $i \leftarrow i + 1$.
until $\|\mathbf{v}_{i+1} - \mathbf{y}\| \leq \epsilon$
Output: $\hat{\mathbf{v}} \leftarrow \mathbf{v}_{i+1}$

$\text{NRMSE} := \|\hat{\mathbf{v}} - \mathbf{v}\| / \|\mathbf{v}\|$, where $\hat{\mathbf{v}}$ is the returned estimate and $\mathbf{v}$ the true voltage profile.

Different legacy meter measurements and voltage profiles were generated using MATPOWER [13]. The WLS Gauss-Newton method was implemented using the SE function 'doSE.m' in MATPOWER, while the proposed scheme and the SDR-based one utilized the MATLAB-based optimization modeling package YALMIP [14] along with the interior-point solver SeDuMi [15] on an Intel CPU @ 3.4 GHz (32 GB RAM) computer. Furthermore, the flat-voltage profile (i.e., all-ones vector) point is used to initialize the Gauss-Newton iterations and the FPP-based SE scheme. In order to fix the phase ambiguity, the phase at the reference bus is set to 0 in all tests.

The first experiment on the IEEE 30-bus benchmark system simulates the noisy measurement scenario [5,16]. The actual voltage magnitude of each bus was Gaussian distributed with zero-mean and variance 0.01, while its angle was uniform over $[-0.3\pi, 0.3\pi]$. The schemes were tested on 500 Monte Carlo realizations. All voltage magnitudes as well as all active and reactive power flows were measured. Independent zero-mean Gaussian noise was assumed having standard deviation 0.02 for power meters and 0.01 for voltage measurements [5]. Among the 500 Monte Carlo runs, the Gauss-Newton method diverged 2 times. The SDR estimator was recovered from the SDR solution by picking the minimum-cost vector over the eigenvector and 50 randomizations. Fig. 1 compares the magnitude and angle estimation errors of three SE schemes across buses. The curves in Fig. 1 demonstrate the efficacy of the FPP-based SE solver, in this high-SNR, complete-data scenario. Regarding running time, the Gauss-Newton scheme converges in 0.2 seconds typically, while the SDR-based and the FPP-based methods take 10 and 15 seconds on average, respectively.

To test the robustness of the proposed SE scheme, the second experiment entails the IEEE 57-bus test feeder and a varying number of noisy measurements [16]. Each bus had its actual voltage magnitude uniformly distributed over $[0.9, 1.1]$ and its angle over $[-0.1\pi, 0.1\pi]$. The measurements were randomly and uniformly sampled from each type of measurements. Considering for example the active power injections, the maximum number of active injection is equal to the number of buses N. Upon introducing a measurement ratio

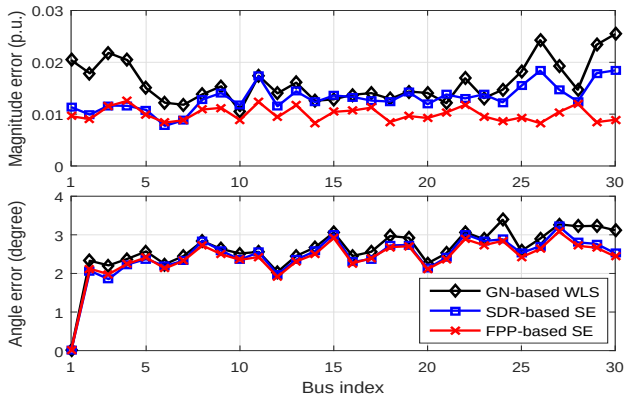

Fig. 1. Magnitude and angle estimation errors at different buses on the IEEE 30-bus system using: i) Gauss-Newton based WLS; ii) SDR-based SE; and iii) FPP-based SE.

$\gamma \in [0.1, 1]$, each realization sampled independently and uniformly $\lfloor \gamma N \rfloor$ out of N active power injections measurements; and likewise for all other types of measurements. Measurement noise was randomly and independently generated from Gaussian distribution having zero-mean and standard deviations 0.01 and 0.03 times their actual values for voltage magnitudes and power injections/flows, respectively. The reported empirical results were obtained by averaging over 100 Monte Carlo realizations. The NRMSE versus γ is shown in Fig. 2, corroborating the robustness of our FPP-based SE.

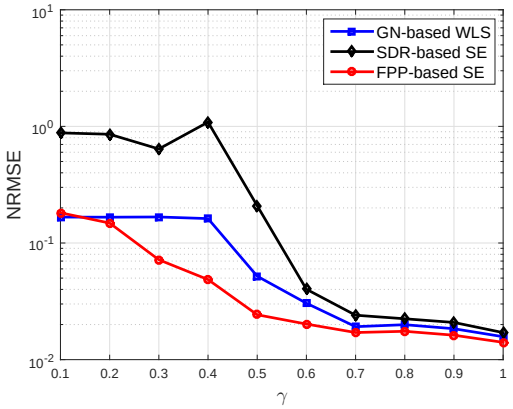

Fig. 2. NRMSE vs γ on the IEEE 57-bus system using: i) Gauss-Newton based WLS; ii) SDR-based SE; and iii) FPP-based SE.

5. CONCLUDING REMARKS

Motivated by the inherent nonconvexity challenge of SE and building on recent advances in handling nonconvex QCQPs, this paper first reformulated the WLS SE task as a nonconvex QCQP, which was then tackled using the FPP algorithm. Simulated tests demonstrated improved performance of our FPP-based SE over its competing Gauss-Newton based WLS and SDR-based SE alternatives.

6. REFERENCES

[1] F. C. Schweppe, J. Wildes, and D. Rom, "Power system static state estimation: Parts I, II, and III," *IEEE Trans. Power App. Syst.*, vol. 89, pp. 120–135, Jan. 1970.

[2] G. B. Giannakis, V. Kekatos, N. Gatsis, S.-J. Kim, H. Zhu, and B. Wollenberg, "Monitoring and optimization for power grids: A signal processing perspective," *IEEE Signal Process. Mag.*, vol. 30, no. 5, pp. 107–128, Sept. 2013.

[3] V. Kekatos and G. B. Giannakis, "Distributed robust power system state estimation," *IEEE Trans. Power Syst.*, vol. 28, no. 2, pp. 1617–1626, May 2013.

[4] V. Kekatos, G. Wang, A. J. Conejo, and G. B. Giannakis, "Stochastic reactive power management in microgrids with renewables," *IEEE Trans. Power Syst.*, vol. 30, no. 6, pp. 3386–3395, Nov. 2015.

[5] H. Zhu and G. B. Giannakis, "Power system nonlinear state estimation using distributed semidefinite programming," *IEEE J. Sel. Topics Signal Process.*, vol. 8, no. 6, pp. 1039–1050, Dec. 2014.

[6] D. P. Bertsekas, *Nonlinear Programming*, 2nd ed. Belmont, MA: Athena Scientific, 1999.

[7] S.-J. Kim, G. Wang, and G. B. Giannakis, "Online semidefinite programming for power system state estimation," in *Proc. IEEE Conf. on Acoustics, Speech and Signal Process.*, Florence, Italy, May 2014, pp. 6024–6027.

[8] G. Wang, S.-J. Kim, and G. B. Giannakis, "Moving-horizon dynamic power system state estimation using semidefinite relaxation," in *Proc. IEEE PES General Meeting*, Washington, DC, July 2014, pp. 1–5.

[9] O. Mehanna, K. Huang, B. Gopalakrishnan, A. Konar, and N. D. Sidiropoulos, "Feasible point pursuit and successive approximation of non-convex QCQPs," *IEEE Signal Process. Lett.*, vol. 22, no. 7, pp. 804–808, Nov. 2015.

[10] A. S. Zamzam, N. D. Sidiropoulos, and E. Dall'Anese, "Beyond Relaxation and Newton-Raphson: Solving AC OPF for Multi-phase Systems with Renewables," *IEEE Trans. Smart Grid*, 2016 (under revision).

[11] J. Lavaei and S. Low, "Zero duality gap in optimal power flow problem," *IEEE Trans. Power Syst.*, vol. 27, no. 1, pp. 92–107, Feb. 2012.

[12] P. M. Pardalos and S. A. Vavasis, "Quadratic programming with one negative eigenvalue is NP-hard," *J. Global Optim.*, vol. 1, no. 1, pp. 15–22, 1991.

[13] R. D. Zimmerman, C. E. Murillo-Sanchez, and R. J. Thomas, "MATPOWER: Steady-state operations, planning and analysis tools for power systems research and education," *IEEE Trans. Power Syst.*, vol. 26, no. 1, pp. 12–19, Feb. 2011.

[14] J. Lofberg, "A toolbox for modeling and optimization in MATLAB," in *Proc. of the CACSD Conf.*, 2004. [Online]. Available: http://users.isy.liu.se/johanl/yalmip/

[15] J. F. Sturm, "Using SeDuMi 1.02, a MATLAB toolbox for optimization over symmetric cones," *Optim. Method Softw.*, vol. 11, no. 1-4, pp. 625–653, Jan. 1999.

[16] Power systems test case archive. Univ. of Washington. [Online]. Available: http://www.ee.washington.edu/research/pstca.